Journal of Power Sources 271 (2014) 305–311

Contents lists available at ScienceDirect

Journal of Power Sources

journal homepage: www.elsevier.com/locate/jpowsour

Anti-fouling response of gold–carbon nanotubes composite for enhanced ethanol electrooxidation

R.S. Sai Siddhardha [a], Manne Anupam Kumar [a], V. Lakshminarayanan [b], Sai Sathish Ramamurthy [a, *]

[a] Department of Chemistry, Sri Sathya Sai Institute of Higher Learning, Prashanthi Nilayam, 515134, India
[b] Soft Condensed Matter Group, Raman Research Institute, C.V. Raman Avenue, Bangalore 560080, India

HIGHLIGHTS

- Surfactant free laser ablation synthesis of gold–carbon nanotubes nanocomposite.
- Catalytic modification of carbon paste electrode for ethanol electrooxidation.
- Remarkable stability of the catalyst towards electrooxidation.
- Low Arrhenius energy for electrooxidation of ethanol (~28 kJ mol^{-1}).
- Auto depassivation effect on intermediates by the electrocatalyst.

GRAPHICAL ABSTRACT

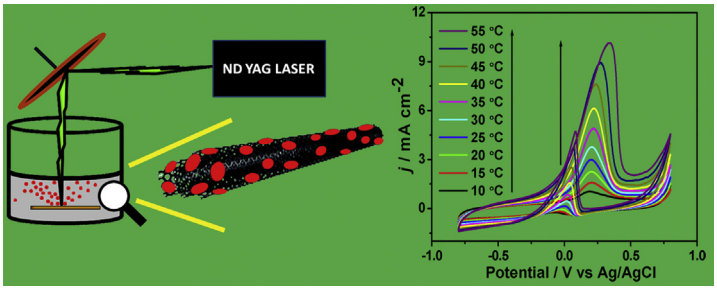

ARTICLE INFO

Article history:
Received 28 June 2014
Received in revised form
3 August 2014
Accepted 4 August 2014
Available online 12 August 2014

Keywords:
Ethanol electrooxidation reaction
Laser ablation
Gold carbon nanotubes
Anti-fouling
Surface de-passivation
Fuel cells

ABSTRACT

We report the synthesis of gold carbon nanotubes composite through a one-pot surfactant free approach and its utility for ethanol electrooxidation reaction (EOR). The method involves the application of laser ablation for nanoparticle synthesis and simultaneous assembly of these on carbon nanotubes. The catalyst has been characterized by field emission scanning electron microscopy (FESEM), energy dispersive X-ray analysis (EDAX) and UV–vis spectroscopic techniques. A systematic study of gold carbon nanotubes modified carbon paste electrode for EOR has been pursued. The kinetic study revealed the excellent stability of the modified electrode even after 200 cycles of EOR and with an Arrhenius energy as low as ~28 kJ mol^{-1}. Tafel slopes that are the measure of electrode activity have been monitored as a function of temperature of the electrolyte. The results indicate that despite an increase in the reaction rate with temperature, the electrode surface has not been significantly passivated by carbonaceous species produced at high temperatures.

1. Introduction

Kinetics of ethanol oxidation reaction (EOR) has been widely studied on platinum in alkaline medium [1–4]. The two main reasons for this extensive research in EOR are: (i) Ethanol is a safer substitute to hydrogen in fuel cell applications and (ii) Active catalytic behaviour of platinum [5]. Although platinum has been the preferred catalytic material, the search for newer anode catalysts is still ongoing, since Pt is expensive and its surface gets poisoned by carbonaceous species produced during EOR [3]. Therefore, the quest for studying EOR on different metal surfaces and nanocomposites with less poisoning & superior catalytic activity is desirable [6]. Gold nanoparticles (AuNPs) in this context, when

* Corresponding author. Tel.: +91 8790314405; fax: +91 8555286919.
E-mail addresses: saisiddhardha@sssihl.edu.in, rssaisiddhardha@gmail.com (R.S. Sai Siddhardha), rsaisathish@sssihl.edu.in (S.S. Ramamurthy).

http://dx.doi.org/10.1016/j.jpowsour.2014.08.023
0378-7753/

loaded over heterogeneous supports, have wide applications pertaining to catalysis and electro catalysis [7,8]. The reports on the kinetics of EOR on AuNPs supported composites have however been sparse. One such study pursued by Rodriguez et al. describes the superior activity of gold in alkaline medium owing to the crucial role of CO [9,10]. More recently, Pandey et al. have studied the electrocatalytic activity of AuNPs on conducting polymers (Au-CPs) like polyaniline (PANI), polypyrrole (PPY), polythiophene (PTP) and poly(3,4-ethylenedioxythiophene) (PEDOT) [11]. These studies have broadened the scope for pursuing the kinetics of EOR with AuNPs based catalytic composites. There are several reports on the use of carbon nanotubes as ideal supports, on account of their high electrical conductivity; surface area; mechanical strength; and chemical stability [12]. An extension to this has been the synergistic use of AuNPs supported on carbon nanotube (CNT) scaffolds, having the dual properties of the individual entities [13].

Of the several routes available for AuNPs synthesis, the bottom up route is very well known. This approach gives precise control over the size and shape of the synthesized particles [14,15]. Nevertheless, the capping agents may mask the catalytic performance of the nanoparticle by hindering the approach of the reactant species towards the metal surface and reduce the efficiency of the catalysis [16]. Therefore, an alternative top down route for synthesis has already been explored by a number of researchers. These methods involve electrochemical [17], microwave [18], sonochemical [19] and ball-milling techniques [20], in sequel to the earlier work that involves the synthesis of AuNPs in water through laser ablation (LA). In the present study we have employed LA approach not only to synthesize AuNPs, but also to decorate them over multi walled CNTs (MwCNTs). In this study, Au-CNT composite is synthesized in a single step one-pot reaction without the use of any surfactants. To attain an appreciable loading of AuNPs over MwCNTs, the MwCNTs must be homogeneously dispersed in water. This dispersion has been made possible due to the uniform functionalization of CNTs achieved through a microwave induced reaction [3]. In the recent past, we have loaded NPs over functionalized hydrogen exfoliated graphene using LA and used it as a catalyst for EOR and environmental remediation involving the reduction of coloured dyes [21]. In the present study, carbon paste electrode (CPE) has been modified using Au-CNT and has shown excellent catalytic performance for ethanol electrooxidation in alkaline medium. A high rate of electro–catalytic activity has been observed using Au-CNTs with a decreased activation energy (AE) barrier. The AE for EOR with Au-CNTs is ~28 kJ mol^{-1}. The electrode has shown excellent stability even after 200 cycles of ethanol oxidation. These properties make the composite a plausible contender for direct ethanol fuel cell (DEFC) and other analogous applications. The hybrid catalyst material has been characterized by field emission scanning electron microscopy (FESEM), energy dispersive X-ray analysis (EDAX) and UV–vis spectroscopy.

2. Experimental section

2.1. Reagents

MwCNTs (OD 20–30 nm, purity 95%) were purchased from Cheap tubes Inc. All the other chemical reagents used in this study were of analytical grade. All the aqueous solutions in this study were prepared with Millipore water having resistivity of 18.2 Ω-cm.

2.2. Instruments

The UV–vis spectra were recorded using a shimadzu 2450 PC UV–vis spectrophotometer equipped with a quartz cuvette holder for liquid samples. FESEM and EDAX were obtained from FESEM (Zeiss). Functionalization of CNTs was done using microwave accelerated reaction system (mode: CEM Mars) with internal temperature and pressure controls. A high power nanosecond Nd:

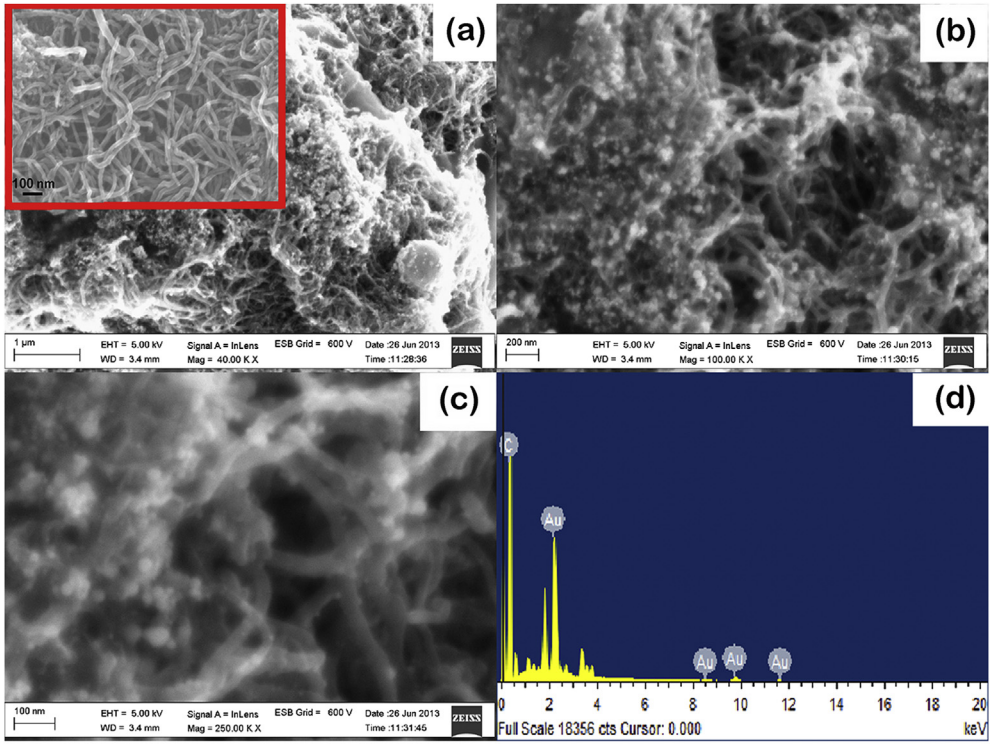

Fig. 1. (a) to (c) FESEM images of Au-CNT under different magnifications. (d) shows the EDAX Spectrum of Au-CNT. Inset in (a) shows FESEM image of pristine MwCNT.

YAG (Surelite III) laser with its fundamental harmonic at 1064 nm was used as the irradiation source to synthesize Au-CNT. A conventional 3 electrode set up was used for all the electrochemical studies. All voltammetric and chronoamperometric measurements were carried out using Ivium compactstat, a potentiostat/galvanostat equipped with a temperature controller (Julabo Model F 25).

2.3. Laser ablation mediated synthesis (LAMS) of Au-CNT

MwCNTs were functionalized based on previous reports [3] to yield carboxylated multi walled CNTs (MwCNT-COOH). In brief, purified MwCNTs were weighed and treated with a mixture of sulphuric & nitric acid under microwave radiation for 20 min at 140 °C. The generation of surface oxygen functionalizations lead to high aqueous dispersibility. The solid was filtered with a 10 μm membrane filter, rinsed with water to neutral pH and dried to 80 °C under vacuum to a constant weight.

An aqueous dispersion of MwCNT-COOH was prepared by dispersing 1 mg in 25 ml of water. A gold strip of (2 cm × 1 cm) was cleaned ultrasonically in 10 ml piranha solution (caution) and placed in a 25 ml beaker containing 3 ml aqueous dispersion of MwCNT-COOH. A nanosecond Nd: YAG (Surelite III) of high power at 1064 nm was used as an irradiation source for the gold strip ablation. The laser was optically steered through a convex lens onto the gold strip. The laser pulse energy was 50 mJ with a repetition rate of 10 Hz and the focal length was 10 cm. All the conditions were kept constant throughout the experiment. The ablation was continued for 40 min and the weight loss of the gold strip was found to be 0.3 mg. Likewise the gold strip was also ablated in water to get an aqueous dispersion of AuNPs and the weight loss was 1.3 mg.

2.4. Preparation of Au-CNT modified CPE

Au-CNT modified CPE was prepared by a slight modification to the conventional fabrication [3]. 50 mg of graphite powder was homogenously grinded with 18 μl of paraffin oil. The resultant paste was compactly stuffed into the CPE and the exposed surface was carefully smoothened. 50 μl of the catalyst was drop cast layer by layer in aliquots of 10 μl and dried at room temperature for further use. The CPE prepared then was used in acidic as well as in alkaline medium to study the electrooxidation reactions. To ensure the purity and replicable condition of the electrode, prior to each experiment, CPE was washed with millipore water and amperometrically treated with a positive potential of 1.2 V, followed by a programmed negative potential of −0.4 V. This process oxidizes the modified electrode surface and is accompanied by the removal of the adsorbed impurities. This ensures the regeneration of the electrode surface prior to every experimental step. The CNT modified electrode that was used as a control was also prepared by the same procedure.

3. Results and discussion

3.1. Characterization of Au-CNT using FESEM, EDAX and UV–vis spectroscopy

The distribution of the nanoparticles over tubular CNT network is evident from the FESEM images with increasing resolution from Fig. 1a–c. The nanoparticles are approximately 20–30 nm in diameter. The EDAX spectrum of the nanocomposite clearly indicates the characteristic gold peaks as seen in Fig. 1d. The excluded peaks belong to the ITO background. The normalized elemental analysis data of Au-CNT obtained from the EDAX with the exclusion of ITO background is presented in Table 1. The wt. % of gold loading on CNT is calculated to be 31.2% whereas the wt. % of carbon is found to be 60.4%. This gives an approximate estimate of the amount of gold present on the nanocomposite.

Table 1
EDAX elemental analysis of Au-CNT.

Element	wt. %	at. %
C K	60.45	88.72
O K	7.15	7.88
Cl K	1.23	0.61
Au M	31.17	2.79
Total	100	100

The UV–vis spectrum of CNTs before and after 5 min of laser ablation of the gold strip can be seen in Fig. 2a. The MwCNT-COOH has shown an extended broad peak between 233 nm and 265 nm corresponding to $\pi-\pi^*$ transition of aromatic C=C bonds. The laser ablation of the gold strip has not only resulted in ablating AuNPs but also in the deoxygenation of the MWCNT-COOH. This is evident with the complete red shift of this broad peak to 265 nm. There is also an emergence of the AuNP absorption at 520 nm. The UV–vis spectrum profile of Au-CNT dispersion with increasing times of laser ablation is presented in Fig. 2b. The increase in the 520 nm peak with an increase in ablation times is indicative of the increased loading of AuNPs over the CNT. All these results clearly demonstrate the supporting of AuNPs over CNTs.

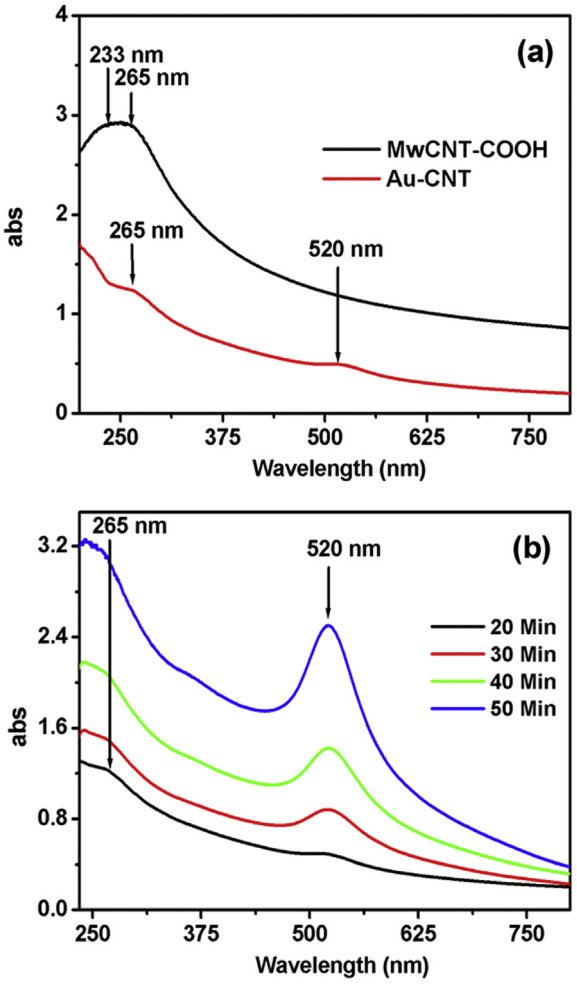

Fig. 2. (a) UV–vis spectra of MwCNT-COOH and Au-CNT before and after 5 min of laser ablation (b) UV–vis spectra overlay of Au-CNT at different ablation times.

3.2. Voltammetric behaviour of Au-CNT modified CPE in acid medium and its EOR in alkaline medium

We have examined the electrocatalytic activity of Au-CNT by studying the EOR of ethanol in 0.5 M NaOH alkaline medium. To confirm that the activity is solely due to the nanocomposite, we even carried out a control experiment with a bare gold electrode that has shown no significant activity. The effective catalytic surface area (ECSA) of the catalyst is calculated by measuring the area under the reduction current curve in Fig. 3a. ECSA indicates the electrochemically accessible active sites on the catalyst. All current values are corrected with respect to ECSA of the catalyst. The EOR with the different catalytic fabrications of the electrode is presented in Fig. 3b. The catalytic activity was found to be larger with the composite than the control in the experiment. The cyclic voltammograms (CVs) of the catalyst at the 1st and 200th cycle are shown in Fig. 3c. The CVs are similar without any significant change indicating the stability and reproducibility of the catalyst material. The details of the onset and peak potentials along with peak currents are presented in Table 2.

In this study, Au-CNT has comparable onset and peak potentials but relatively higher currents than Au-CPs. This indicates that the combination of CNTs with AuNPs acts as a better conducting support than the usage of CPs. The CVs of the Au-CNT electrode at different ethanol concentrations is presented in Fig. 3d. In all of the CV's there is a secondary oxidation peak during the reverse scan. This reverse anodic peak can be attributed to the inability of the surface gold atoms to equilibrate with the lattice atoms after the reduction of blocking oxide film. This consequently leads to the superior catalytic activity by the exposed high energy sites.

The much familiar reaction mechanism for the oxidation of ethanol in alkaline medium involves the conversion of ethanol into acetate ions at the anode. The various reaction steps have been summed up in Scheme 1 based on the previous spectro-electrochemical investigations. [22].

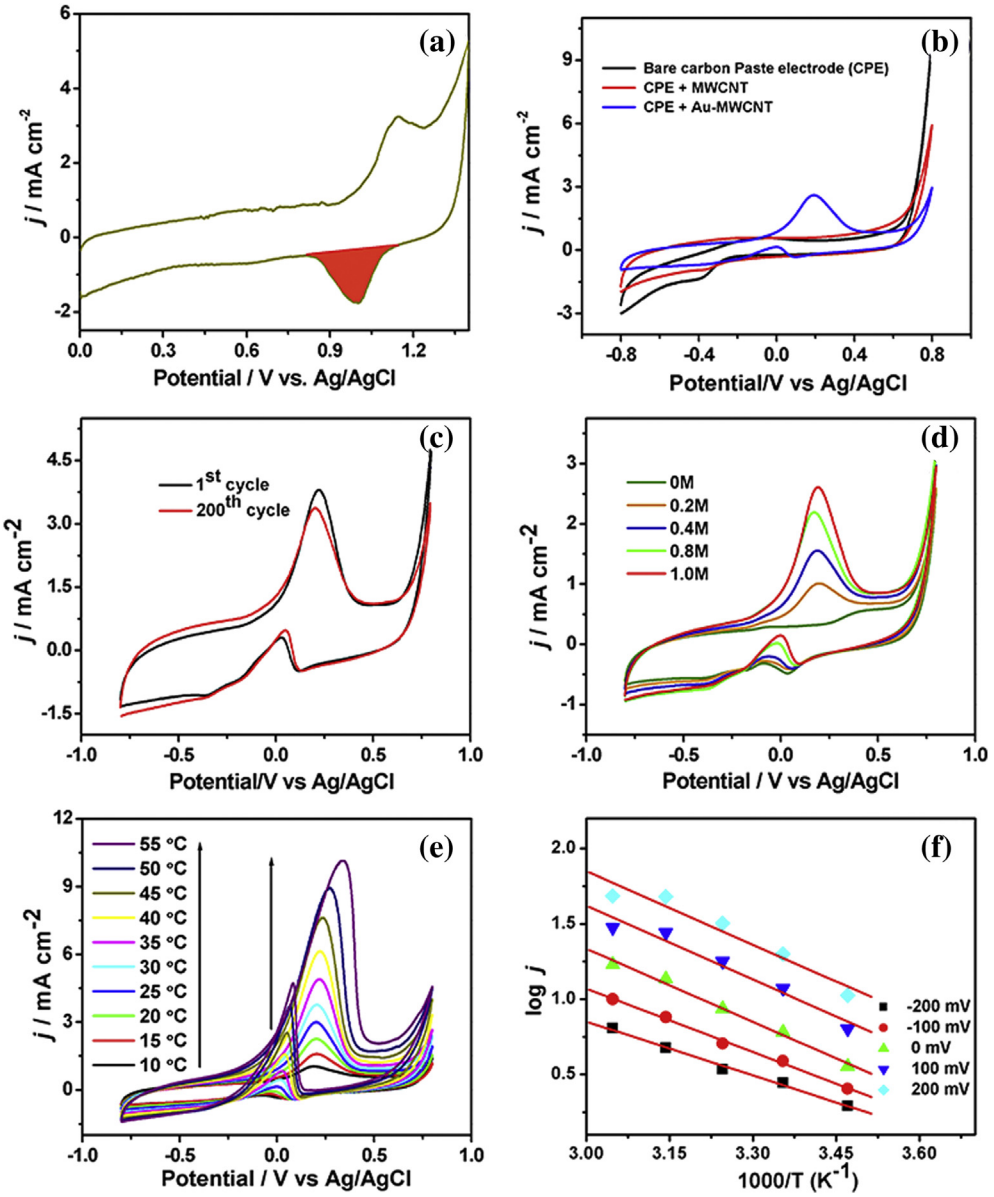

Fig. 3. (a) CV of Au-CNT modified CPE in 0.5 M H_2SO_4 solution (b) CV overlay of bare CPE, MwCNT, Au-CNT (c) The 1st and 200th CVs for Au-CNT modified CPE in 1M ethanol in 0.5M NaOH. (d) CV overlay of EOR in 0.5 M NaOH solution for different ethanol concentrations (e) CV overlay of Au-CNT for EOR in 1M ethanol in 0.5 M NaOH at different temperatures (f) Arrhenius plots of EOR using Au-CNT at various potentials. Scan rate: 50 mV s^{-1}.

Table 2
Comparison of the onset potentials, peak potentials and peak currents in EOR using Au-CNT and earlier report.

Nano composite	Onset potential (V)		Peak potential (V)		Peak current (mA cm^{-2})		Ref.
	1st cycle	200th cycle	1st cycle	200th cycle	1st cycle	200th cycle	
Au-CNT	−0.13	−0.14	0.22	0.20	3.79	3.37	[This study]
Au-PANI	−0.34	−0.34	0.31	0.28	3.36	3.50	[11]
Au-PPY	−0.35	−0.40	0.14	0.12	2.02	2.00	
Au-PTP	−0.40	−0.40	0.17	0.20	1.63	1.60	
Au-PEDOT	−0.36	−0.36	0.11	0.12	2.93	2.90	

3.3. Determination of activation energy and Tafel plot analysis for EOR

The CVs for EOR at various temperatures are represented in Fig. 3e. The clear shift in the onset potentials is indicative of the low activation energy barrier for ethanol electrooxidation at elevated temperatures. The initial steps for EOR involve the OH^- adsorption on the gold surface, as established in the earlier reports [9]. This OH_{ads} is in fact responsible for achieving high currents for EOR. The electrocatalyst fouling however, occurs on account of the carbonaceous species that are eventually generated during the course of the EOR that block the catalytically active sites. At this juncture, OH_{ads} scavenges the generated carbonaceous species and improves the EOR current [22,23]. The low onset potentials at elevated temperatures are indicative of the enhanced adsorption of the hydroxyl ions onto the gold surface [9,24]. The reverse anodic current increased with the increasing temperature. This can be reasoned to be due to the presence of more catalytically active sites or high energy gold centres at elevated temperatures that fail to equilibrate with their metallic lattice. The Arrhenius plots between log j and 1000 T^{-1} are presented in Fig. 3f. The linear relationship in these plots suggests that the mechanism essentially remains the same at all studied temperatures.

The slope of the Arrhenius plots gives the activation energy (E_a) where the slope (s) = $-E_a$/2.303R. The average activation energy value obtained for Au-CNT is 28.6 kJ mol^{-1} whereas for Au-PANI, Au-PPY, Au-PTP, Au-PEDOT it is 37.0, 56.7, 57.0 and 56.7 kJ mol^{-1} respectively. This reflects the much lesser average E_a value of Au-CNT when compared to the Au-CPs. The relatively low activation energy can be accounted for, by two explanations i.e. (i) the anti-fouling efficiency of Au-CNT during the EOR [25] (ii) the enhanced kinetic rate of EOR due to the presence of catalytically active nanoparticles present on a porous tubular network of CNT as seen in the FESEM images Fig. 1. Although the AuNPs are the same on both the CNTs and CPs, the low activation energy in our work is conclusive that CNTs provide a better support for AuNPs than CPs. The E_a value obtained in the current study is comparable to the earlier reported Pt, Pd and Au systems [26].

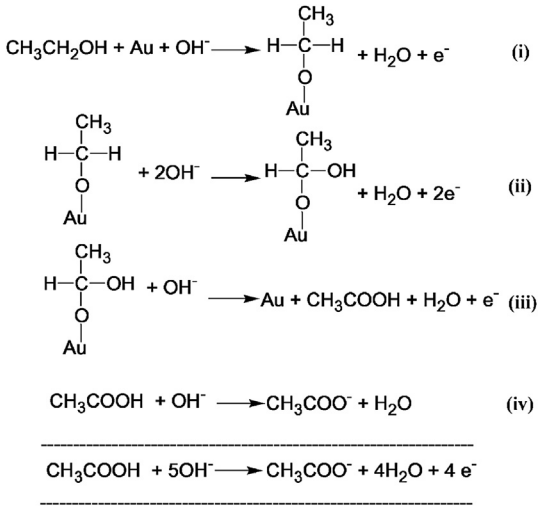

Scheme 1. The mechanism of EOR on the gold electrode in alkaline medium.

The Tafel slopes at various temperatures are presented from Fig. 4a–e. The corresponding slope values are presented in Table 3. Tafel slopes are essentially plots of polarization and are suggestive of the reaction mechanism. In case of alcohol oxidation, these plots however, are complicated on account of the adsorption of the carbonaceous intermediates resulting in the surface poisoning. This results in the non-linearity of the Tafel slope for EOR [27]. Nevertheless, Tafel slopes are indicators that provide a wider perspective about the reaction process and the temperature dependency of the EOR [28]. The data obtained in the present study reveals two distinct slopes, with the second slope values being higher than the first. Since the variation of current with the overpotential is also indicative of the availability of the free surface sites on the electrode, one can relate the Tafel slope to the extent of surface contamination during the course of the reaction. A change in the Tafel slope with temperature is indicative of the degree of adsorption of the impurities on the Au-CNT surface as the reaction progresses. In an earlier study [11], using Au-CP nanocomposite film electrode, the increasing Tafel slope values increased with increasing temperature, that has been attributed to the increased passivation of the electrode surface by means of carbonaceous impurities. These adsorbed carbonaceous impurities block the active centres during the EOR. But in the present study, there is a distinct decrease in the Tafel slopes, which is due to an increase in the EOR currents with an increasing temperature. This decrease in the surface passivation with increasing temperature on the Au-CNT modified electrode surface when compared to the Au-CP modified film electrode is evidently an advantage of the present nanocomposite system. The reduced passivation effect of Au-CNT surface also correlates well with the lower activation energy of the system when compared to the Au-CP as discussed earlier. This highlights the auto depassivation ability of the Au-CNT modified CPE towards EOR.

A plot between log$I$ and log$c$ (ethanol concentration) that gives the order of the reaction is presented in the Supporting information Fig. S1. [29]. The following Eq. has been used to calculate the order for EOR [26].

$$\log I = \log nFk + m \log c$$

where F is the Faraday constant, k is the reaction constant, m is the order of the reaction and c is the concentration of ethanol. At any constant temperature, the slope of the plot gives the apparent order of the reaction (m) with respect to the concentration of ethanol. We have studied the order of the reaction at 0.0 V and 0.1 V for different ethanol concentrations and found it to be 0.4 and 0.54 respectively. There is a slight change in the reaction order at the selected potentials. The reaction order is low at lower potentials (0.4 V) and slightly high at higher potential (0.54) as shown in Fig. S1. This

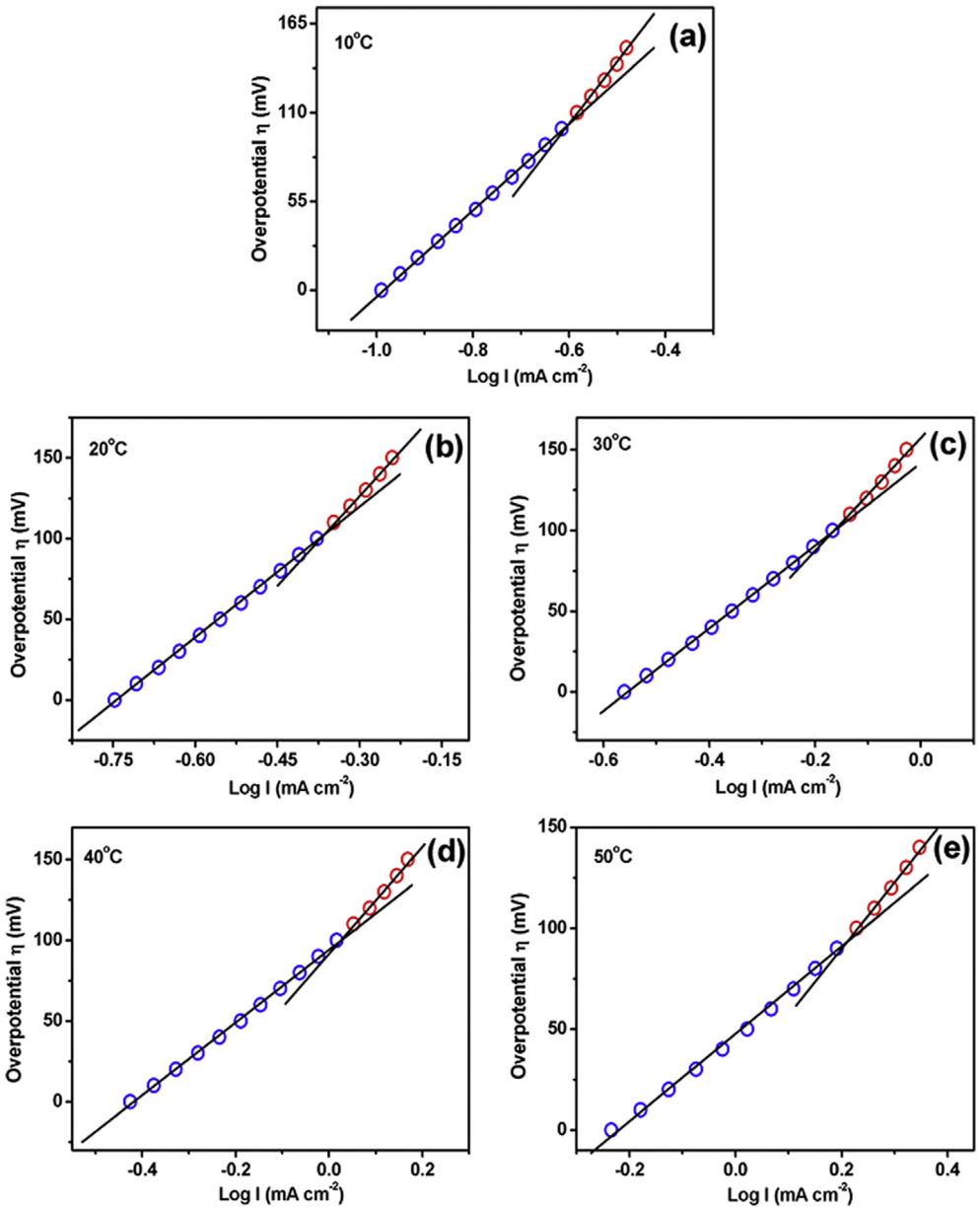

Fig. 4. Tafel plots at different temperatures.

shows the dynamic nature of the mechanism as we move on from lower to higher potentials.

4. Conclusion

The present study has devised a surfactant free synthesis of Au-CNT through the LAMS approach. The catalyst has shown excellent stability towards electrooxidation of ethanol even after 200 CVs. The kinetic study of EOR in alkaline medium using the as-synthesized Au-CNT has shown a significantly low Arrhenius energy of ~28 kJ mol^{-1}. Tafel studies indicate the improved efficiency of the catalyst with increasing temperature, on account of the reduced fouling of the modified electrode surface. This signifies the auto depassivation ability of Au-CNT towards EOR and also highlights it as a plausible contender for use as a catalyst material in fuel cells. We intend to extend this surfactant free approach to graphene based materials as catalysts for electrooxidation of other small organic molecules.

Table 3
Tafel slope values at different temperatures.

Temperature (°C)	Tafel slope values	
	1st slope	2nd slope
10	264.4	384.6
20	269.9	371.3
30	254.7	372.6
40	226.2	341.7
50	215.5	332.4

Acknowledgements

The authors are thankful to Prof. Somenath Mitra for providing gratis sample of functionalized CNTs, to Anu Renjith, Doctoral researcher, RRI, for her help in conducting the electrochemical

studies and to Dr. Sai Muthukumar V, Dept. of Physics, SSSIHL for providing access to use the laser facility. SSR and RSSS acknowledge the funding from DBT Ramalingaswami fellowship and UGC JRF fellowship, Govt. of India respectively. The authors convey special thanks to Sri Prashant Luthra, Dept. of English, SSSIHL, Sri Chelli Sai Manohar, Dept. of Chemistry, SSSIHL for the proof reading of the manuscript and Prof. Chelli Janardhana, Dept. of Chemistry, SSSIHL for his timely suggestions. The authors are grateful to Bhagawan Sri Sathya Sai Baba for his constant inspiration.

Appendix A. Supplementary data

Supplementary data related to this article can be found at http://dx.doi.org/10.1016/j.jpowsour.2014.08.023.

References

[1] E. Antolini, J. Power Sources 170 (2007) 1–12.
[2] A. Arico, P. Creti, P. Antonucci, V. Antonucci, Electrochem. Solid State Lett. 1 (1998) 66–68.
[3] L. V Kumar, S. Addo Ntim, O. Sae-Khow, C. Janardhana, V. Lakshminarayanan, S. Mitra, Electrochim. Acta 83 (2012) 40–46.
[4] J. Wang, S. Wasmus, R. Savinell, J. Electrochem. Soc. 142 (1995) 4218–4224.
[5] W. Zhou, Z. Zhou, S. Song, W. Li, G. Sun, P. Tsiakaras, Q. Xin, Appl. Catal. B 46 (2003) 273–285.
[6] A. Serov, C. Kwak, Appl. Catal. B 90 (2009) 313–320.
[7] J. Huang, X. Han, D. Wang, D. Liu, T. You, ACS Appl. Mater. Interfaces 5 (2013) 9148–9154.
[8] R. Kumar, E. Gravel, A. Hagège, H. Li, D.V. Jawale, D. Verma, I.N. Namboothiri, E. Doris, Nanoscale 5 (2013) 6491–6497.
[9] P. Rodriguez, Y. Kwon, M.T. Koper, Nat. Chem. 4 (2012) 177–182.
[10] Y. Kwon, S.C. Lai, P. Rodriguez, M.T. Koper, J. Am. Chem. Soc. 133 (2011) 6914–6917.
[11] R.K. Pandey, V. Lakshminarayanan, Appl. Catal. B 125 (2012) 271–281.
[12] H.-B. Zhang, X.-L. Liang, X. Dong, H.-Y. Li, G.-D. Lin, Catal. Surv. Asia 13 (2009) 41–58.
[13] P.V. Dudin, P.R. Unwin, J.V. Macpherson, Phys. Chem. Chem. Phys. 13 (2011) 17146–17152.
[14] M.-C. Daniel, D. Astruc, Chem. Rev. 104 (2003) 293–346.
[15] Y. Xia, N.J. Halas, MRS Bull. 30 (2005) 338–348.
[16] Z. Niu, Y. Li, Chem. Mater. 26 (2013) 72–83.
[17] S. Singh, D.V.S. Jain, M.L. Singla, Anal. Methods 5 (2013) 1024–1032.
[18] M. Tsuji, M. Hashimoto, Y. Nishizawa, M. Kubokawa, T. Tsuji, Chem. Eur. J. 11 (2005) 440–452.
[19] K. Okitsu, M. Ashokkumar, F. Grieser, J. Phys. Chem. B 109 (2005) 20673–20675.
[20] J.F. de Carvalho, S.N. de Medeiros, M.A. Morales, A.L. Dantas, A.S. Carriço, Appl. Surf. Sci. 275 (2013) 84–87.
[21] R.S. Sai Siddhardha, V. Lakshman Kumar, A. Kaniyoor, V. Sai Muthukumar, S. Ramaprabhu, R. Podila, A.M. Rao, S.S. Ramamurthy, Spectrochim. Acta Part A 133 (2014) 365–371.
[22] R. De Lima, H. Varela, Gold Bull. 41 (2008) 15–22.
[23] G. Tremiliosi-Filho, E. Gonzalez, A. Motheo, E. Belgsir, J.-M. Léger, C. Lamy, J. Electroanal. Chem. 444 (1998) 31–39.
[24] S.-G. Sun, A.-C. Chen, Electrochim. Acta 39 (1994) 969–973.
[25] E. Habibi, H. Razmi, Int. J. Hydrogen Energy 38 (2013) 5442–5448.
[26] D. Chu, S. Gilman, J. Electrochem. Soc. 143 (1996) 1685–1690.
[27] S.L. Gojković, T. Vidaković, D. Đurović, Electrochim. Acta 48 (2003) 3607–3614.
[28] R.K. Pandey, V. Lakshminarayanan, J. Phys. Chem. C 113 (2009) 21596–21603.
[29] J. Liu, J. Ye, C. Xu, S.P. Jiang, Y. Tong, Electrochem. Commun. 9 (2007) 2334–2339.